Experimental study of seismo-acoustic frequency and flow velocity of debris flow

Sudhan Regmi[1*], *Ko-Fei* Liu[1], and *Shih-Chao* Wei[2]

[1]Department of Civil Engineering, National Taiwan University, Taipei, Taiwan (R.O.C.)
[2]Feng Chia University, Taichung, Taiwan (R.O.C.)

Abstract. Seismo-acoustic wave radiated from debris flows motion is one of the main properties used for its monitoring and detection. Understanding the Seismo-acoustic wave using geophone recordings may give us great insight into the physical process of debris flows such as flow velocity and flow rate. To connect the seismo acoustic observation to the debris flows motion, vibration signal recorded from fixed geophones were analysed. In this study, a small-scale granular flow of volume 0.2 m3 consisting of material with average particle diameter 3.34 mm was simulated in a hydraulic flume with cross section of 0.5 m X 0.5 m through granular bed to simulate the debris flow. A series of three-axis geophones were buried along channel bed to record the vibrations produced by granular flows. The discrete Fourier transform was used to decompose vibrations into frequency spectrum and the weighted non-linear least square regression was adopted to isolate the dominant frequency functions and peak frequency. Meanwhile, the physical parameters including front profile, surface velocity, flow depth and discharge were tracked through video recordings and were compared with respect to isolated peak frequency. Assuming the radiated peak frequency in the moving granular flow is within 20-50 Hz and normally distributed, the isolated peak frequency shift in the fixed geophone location was analysed with the tracked flow parameters. Results shows that the peak frequency shift seems to have a non-linear relation with the surface velocity.

1 Introduction

Heterogeneous and non-uniform flow conditions of the debris flows possess one of the greatest challenges in understanding the characteristics and nature of such flow conditions. Field conditions of debris flows add a lot of unpredictable circumstances which makes it a lot difficult to improve their understanding. Albeit the unpredictable nature of these flows, idealized laboratory experiments and large number of monitoring data have vastly helped to improve the current understanding of these flows.

At present, several techniques exist to monitor, detect, and define debris flow events. These techniques include the use of ground vibrations, image acquisition and hydrological models. However, the warning system of debris flow is significantly based on rainfall thresholds [1] as there is a substantial gap in the theoretical model governing acoustic and image-based systems. Existing studies provide adequate evidence of high correlation between flow condition and energy of ground vibration but falls short to explain the flow mechanism [2]. Present acoustic based monitoring models can successfully detect debris flows after it initiates, but is lacking to define the actual flow characteristics. Nevertheless, detection alone does not correspond to a warning system due to the short time between detection and disaster.

2 Experimental Methodology

This study is based on the detecting and analysing frequencies of acoustic vibration induced by moving debris (granular mass) over a finite media and the flow velocity of the moving debris source. To simulate the debris flow, $0.2\,m^3 \pm 10\%$ of debris material with approximate average diameter (d_{avg}) of 3.34 mm was allowed to flow through a flume with cross section of $0.5\,m \times 0.5\,m$, inclined at an angle of 24°, under influence of gravity assisted by constant flow of water. Simple illustration of experimental setup is shown in Fig. 1 and Fig. 2.

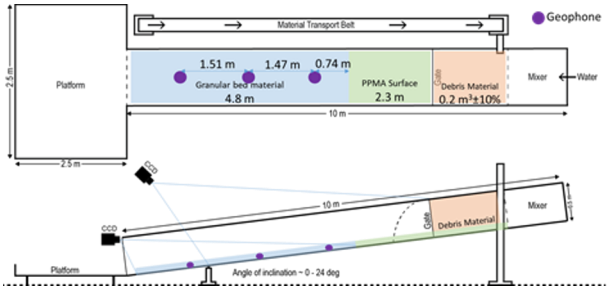

Fig. 1. Semantic sketch for experimental Setup describing the overall setup including the locations of geophones and video cameras

* Corresponding author: sudhan.regmi@gmail.com

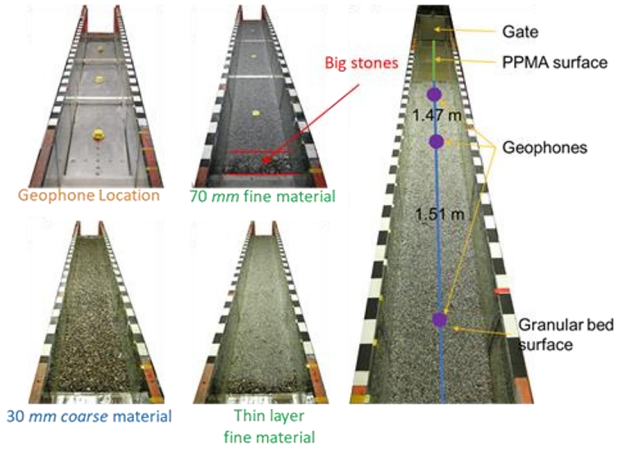

Fig. 2. Stages of flume bed preparation with geophones locations, fine granular material, coarse granular material, final stage with very thin layer of fine granular material on top of coarse material, and the completed flume (right)

The flow region for the simulated debris flow can be separated into three main sections. Initial 2.3 m section after the quick-release gate holding the source material is lined with smooth PPMA material which allows the source material to accelerate before passing through the granular surface. This section can be labelled as the acceleration zone. The granular section after the acceleration zone is constructed to simulate the granular bed surface for debris flow. This section is laid out for the remaining 4.8 m and is constructed in three layers, hand compacted after each layer. The first layer consisted of fine granular material same as the source material with approximate d_{avg} of 3.34 mm, laid at a thickness of 70 mm throughout. The second layer consisted of coarse granular material with approximate d_{avg} of 11.65 mm, laid at a thickness of 30 mm on top of the fine material. This layer of coarse material acts as erosion barrier for the fine material underneath. The third layer consists of very thin layer of fine granular material, same as the first layer on top of the coarse material to reduce the surface friction of the bed. Although, all the 4.8 m section after the acceleration zone is constructed the same, it can still be divided into two sections. The first 3 m section can be labelled as granular-flow zone, where the source material flows freely over the granular bed, deaccelerating constantly due to the surface friction. The remaining 1.8 m section can be labelled as the accumulation zone, where the source material may accumulate at the end of the flume. As the experiment progresses, the accumulation zone may extend to the granular-flow zone based on the volume of source material used.

The acoustic signals/vibrations induced by the moving debris mass is detected and recorded by three geophones, completely buried under the fine granular material, and fixed to the bottom of the flume. These geophones are placed approximately 1.5 m apart from each other with the first one at 3 m from the gate (0.74 m from the end of PPMA surface). The thickness of bed material above the geophones is maintained at 30 mm throughout. In conjunction with geophones video cameras are used to record the progression of the experiment to track the phase speed of the flow front.

In total 4 sets of experiments were performed, with the first three having similar flow conditions but varying water discharge. However, the final experiment was conducted as a dam overflow experiment. In this last experiment, a 300 mm high dam was placed at 2.4m from the start of the granular bed, being all other conditions same as the previous three experiments.

3 Analysis

The frequency analysis part in this study comprises of estimating the frequency response of the flow using the data acquired by geophones. The first step for geophone data preparation is to identify the acquisition parameters. This includes the sampling rate and the unit of sampling of the sampled data. For this study, the sampling rate was 5000 Hz, i.e. a data is sampled every 0.0002 Seconds. After identifying the acquisition parameters, time for the opening of the gate was identified based on the highest peak observed in time series data. When the gate is opened, it hits the flume bed at high force which creates a large peak in the time series data. This large peak also creates additional interfering frequencies undermining the frequencies produced by actual event. Hence, the data for analysis is selected 0.5 seconds after opening of the gate with an assumption that the frequency of the events overpowers the frequency from the gate opening after 0.5 seconds based on observations.

The key characteristic component of the vibration recorded by the geophone can be extracted using appropriate analysis technique. Among various tools available for interpretation of such signals, variants of Fourier transform are used. As the data recorded by the geophone are of discrete nature, discrete Fourier transform (DFT) of overall event duration was performed using the Fast Fourier Transform (FFT) algorithm [3]. In this study the DFT on the event data was performed using Python library, SciPy and NumPy [4].

Similarly, Short-time Fourier transform (STFT), a variant of DFT was used to compute the discrete Fourier series for a short period to analyse the change in frequency spectrum overtime. For this study, STFT we computed for 1 sec data at a time with 96.667% overlap, resulting in time resolution of STFT of 0.033 seconds to be consistent with time resolution of image analysis (i.e. 30 fps).

DFT resolves the frequency in both positive and negative domain, the maximum frequency resolved is half of the sampling frequency call Nyquist frequency. For this study, the sampling frequency is 5000 Hz, hence the maximum frequency resolved is 2500 Hz. Since, we are concerned with the lower frequency range for debris flow, frequency up to 100 Hz is only considered for analysis.

Seismo-acoustic frequency induced by debris flow normally ranges from 10-80 Hz, with lower frequency observed at surge front and higher frequency towards the end [5]. The dominant frequency induced by the flow is generally between 20-50 Hz [6] and higher frequency is normally attributed to water flow. Similar trend was observed from the DFT analysis of experimental data.

Hence, to develop an appropriate model for non-linear regression, the frequency spectrum was expected to be normally distributed among these three frequency clusters. Again, superposition principle of these three normally distributed frequency ranges were presumed to

be valid and could be summed together. Hence, a model for linear summation of three Gaussian distribution was adopted for the non-linear regression analysis. This model can be described as:

$$f(F) = \sum_{n-1}^{3} \alpha_n \exp\left[-\frac{1}{2}\left(\frac{F-\mu_n}{\sigma_n}\right)^2\right] \quad (1)$$

Where, F is the frequency range for analysis, α_n is the amplitude of the function, μ_n is the location of the peak and σ_n is the spread of the distribution.

The Gaussian function have three unknown variables, which results in nine variables considering all three functions. This study is focused on the location of the peak. Although, using weighted non-linear least square regression method, all nine variables are computed. Detection of peak frequencies for one of the experiments for one instant is shown in Fig. 3.

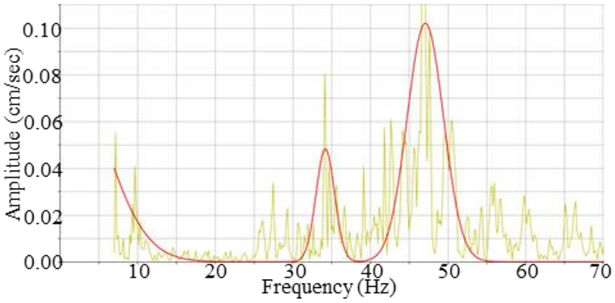

Fig. 3. Detection of peak frequencies using the Gaussian regression

Although all three frequencies in low frequency (10-20), mid frequency (20-50) and higher frequency (50-100) are resolved using the three-peak model, only the frequency in mid-range are considered during the analysis as this range is considered dominant during the debris flow events. Lower frequencies are omitted because the natural frequency of the geophone used in the experiments is 10 $Hz \pm 2.5\%$, this causes maximum resonance in that range and its amplitude cannot be established exclusively for the debris flow movement. Also, the higher frequency is commonly attributed to the water flow, for this reason this range is omitted as well.

Besides the geophone analysis, this study also focuses on physical characteristics of the debris flow including flow velocity, flow depth and discharge. To measure these physical parameters, various image analysis approaches were used on the video taken during the experiments. All experiment proceedings were recorded using for video cameras and recorded at either 60 frames per second or 30 frames per second. To maintain consistency with the analysed geophone data, the time resolution of 30 fps (0.033 sec) was used for image extraction from video files.

Using MATLAB's image processing toolbox [7], first the video file was separated into individual frames. The separated images were then converted into grayscale and using Gaussian filtering lightning inconstancy was removed from each frame. Then, using the principle of perspective projection, the images were transformed into orthographic projection with known X and Y scales. Finally, the front location, particle velocity and flow height were traced on each frame manually, recording the location of each point on the frame for all images. Fig. 4 shows the side profile of the flow during one of the experiments:

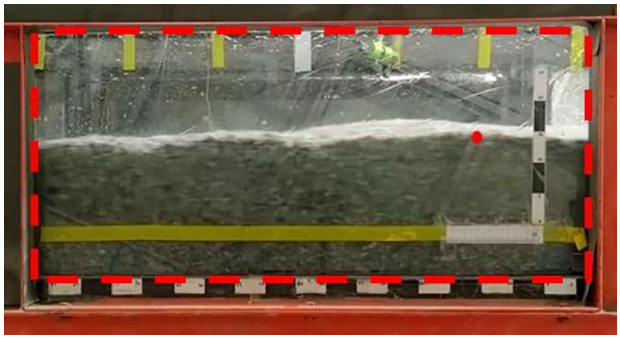

Fig. 4. Side profile of the experiment. The dashed outline indicates ROI for image analysis and the dot indicates the particle being tracked.

The velocity of particles at varying depth was measured for different instances. Due to the varying depth, the measured velocity couldn't be considered as the representative and was converted surface velocity using appropriate velocity profile.

Many studies have observed that the velocity of debris flows is asymmetrical with maximum velocity observed at the surface, decreasing throughout as the flow depth increases [8]. Following the same principle, a non-linear velocity profile with maximum share at the base of the flow and no slip condition was adopted [9], and transformed into non-dimensional flow parameter as:

$$v = (2-\alpha)v_{mean}\left[1-\left(1-\frac{z}{h}\right)^{\frac{1}{1-\alpha}}\right] \quad (2)$$

Where, z is the depth of the particle, h is the total depth of flow, $0 \leq \alpha \leq 1$ controls the shape of the profile by controlling amount of shear within the greater part of the flow and v_{mean} is the depth averaged velocity.

At $z = h$,

$$v_{surface} = (2-\alpha)v_{mean} \quad (3)$$

Hence, equation (2) can be re-written as:

$$v = v_{surface}\left[1-\left(1-\frac{z}{h}\right)^{\frac{1}{1-\alpha}}\right] \quad (4)$$

To estimate the value of α from the experimental observations, four sets of data consisting of three velocity observations each were used. These velocity data were observed at different depth at same time for each set of data. To analyse different sets of data from different experiments together, they were normalised for both depth and velocity with respect to maximum depth and maximum velocity (near the surface) observed at same instant. From the analysis, value of α is estimated to be 0.4899 with coefficient of determination (R2) of 0.977.

4 Results and observations

From the recorded seismo-acoustic data and calculated surface velocity, it was initially observed that the relationship between acoustic frequency of the flow and

its surface velocity is nonlinear and to a point even chaotic. No perceptible linear trend among the experiments were observed.

However, another plot of normalized velocity squared to normalized frequency/velocity for all four experiments, shows a power curve distribution as shown in Fig. 5

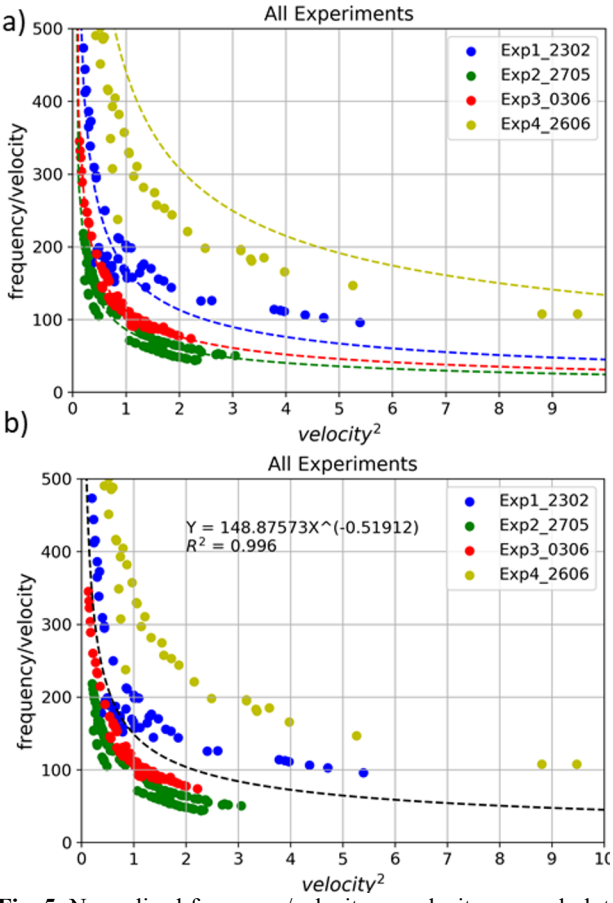

Fig. 5. Normalized frequency/velocity vs velocity squared plot with power curve fit. a) Shows the distribution of all four experiments individually, whereas b) shows the power curve fit for combination of all four experiments.

In the above plot both frequency and velocity are normalised such that:

$$frequency = f\frac{l}{c_0} \tag{5}$$

$$velocity = \frac{c}{c_o} \tag{6}$$

Where, f is the observed frequency, l is the average lenth of flow, c_0 is the average surface velocity of the flow ad c is the observed instantiations surface velocity of the flow. The average length of flow and the average surface velocity of the flow is assumed constant for each experiment. The coefficients and power fit parameter for each experiment is listed in Table 1.

Table 1: Constants and coefficients of power curve fit

	Constant	Power	R^2	l	C_0
Exp_1	115.5026	-0.42843	0.897	2	0.65682
Exp_2	76.0619	-0.55847	0.973	2	1.02158
Exp_3	93.1077	-0.58866	0.993	2	0.77176
Exp_4	587.2582	-0.51905	0.995	2	0.14093
All	128.9883	-0.51925	0.996	2	0.60590

5 Conclusions

Comparing these plots, we can observe that the fitting these data using a power curve in form $Y = aX^n$ shows an exceptional trend with very little amount of scattering. The R^2 value as seen in plots suggests that the data is more suitable for power curve fit than linear fit. Among all these four experiments, experiment 4 plots are slightly different than the rest. This might be due to the different nature of the last experiment as described in previous section. This observation of the frequency and velocity relation could not yet be explained and further analysis and interpretation is necessary.

References

1. H.-Y. Yin, C.-J. Huang, C.-Y. Chen, Y.-M. Fang, B.-J. Lee, T.-Y. Chou, IJEGE, 623-631 (2011)
2. S.-C. Wei, *Theoretical Study of Seismo-acoustic Waves Induced by Debris Flows*, PhD dissertation, NTU, Taiwan (2019)
3. J. W. Cooley, J. W. Tukey, Math. Comput., 297-301 (1965)
4. SciPy-Community, SciPy Ref. Guide, 555-579 (2019)
5. C.-J. Huang, H.-Y. Yin, C.-Y. Chen, C.-H. Yeh, C.-L. Wang, J. Geophys. Res. Earth Surf., **112(F2)**, (2007)
6. R. LaHusen, Debris-flow Hazards and Related Phenomena, 291-304 (2005)
7. MathWorks Inc., Image Processing Toolbox: User's Guide, **R2020a** (2020)
8. Z. Han, G. Chen, Y. Li, W. Wang, H. Zhang, Geomorphology, **241**, 72-82 (2015)
9. C. G. Johnson, B. P. Kokelaar, R. M. Iverson, M. Logan, R. G. LaHusen, J. M. N. T. Gray, J. Geophys. Res. Earth Surf, **117(F1)** (2012)